applied sciences

MDPI

*Article*

# Evaluation of Radioactivity and Heavy Metals Content in a Basalt Aggregate for Concrete from Sicily, Southern Italy: A Case Study

**Francesco Caridi [1,*], Giuseppe Paladini [1], Santina Marguccio [2], Alberto Belvedere [2], Maurizio D'Agostino [2], Maurizio Messina [2], Vincenza Crupi [1], Valentina Venuti [1,*] and Domenico Majolino [1]**

[1] Dipartimento di Scienze Matematiche e Informatiche, Scienze Fisiche e Scienze della Terra, Università degli Studi di Messina, Viale F. Stagno D'Alcontres 31, 98166 Messina, Italy; gpaladini@unime.it (G.P.); vcrupi@unime.it (V.C.); dmajolino@unime.it (D.M.)

[2] Agenzia Regionale per la Protezione dell'Ambiente della Calabria (ARPACal)-Dipartimento di Reggio Calabria, Via Troncovito SNC, 89135 Reggio Calabria, Italy; s.marguccio@arpacal.it (S.M.); a.belvedere@arpacal.it (A.B.); m.dagostino@arpacal.it (M.D.); m.messina@arpacal.it (M.M.)

* Correspondence: fcaridi@unime.it (F.C.); vvenuti@unime.it (V.V.)

**Abstract:** In the present paper, an investigation on the natural and anthropic radioactivity and heavy metals content in a basalt aggregate for concrete from Sicily, Southern Italy, was performed as a case study. In particular, the evaluation of the specific activity of radium-226, thorium-232, potassium-40 and caesium-137 radionuclides was performed by using High-Purity Germanium (HPGe) γ-ray spectrometry, together with the estimation of several indexes developed to evaluate the radiological risk for the population related to radiation exposure, i.e., the alpha index ($I_\alpha$), the radium equivalent activity ($Ra_{eq}$), the absorbed γ-dose rate (D) and the annual effective dose equivalent outdoor ($AEDE_{out}$) and indoor ($AEDE_{in}$). Moreover, measurements of the average heavy metals (arsenic, cadmium, copper, mercury, nickel, lead, antimony, thallium and zinc) concentrations in the analyzed sample were performed by using Inductively Coupled Plasma Mass Spectrometry (ICP-MS). Furthermore, with the aim to investigate any possible chemical pollution, the Enrichment Factor (EF), Geo-accumulation Index ($I_{geo}$), Contamination Factor (CF) and Pollution Load Index (PLI) were assessed. Finally, the identification of the source of the aforementioned radioisotopes of natural origin was carried out by X-ray diffraction (XRD), thus identifying the major mineralogical phases present in the investigated basalt aggregate for concrete.

**Keywords:** basalt aggregate for concrete; radioactivity; radiological risk; mineralogy; HPGe γ-ray spectrometry; heavy metals; pollution; inductively coupled plasma mass spectrometry; X-ray diffraction



**Citation:** Caridi, F.; Paladini, G.; Marguccio, S.; Belvedere, A.; D'Agostino, M.; Messina, M.; Crupi, V.; Venuti, V.; Majolino, D. Evaluation of Radioactivity and Heavy Metals Content in a Basalt Aggregate for Concrete from Sicily, Southern Italy: A Case Study. *Appl. Sci.* **2023**, *13*, 4804. https://doi.org/10.3390/app13084804

Academic Editor: Nikolaos Koukouzas

Received: 13 March 2023
Revised: 4 April 2023
Accepted: 8 April 2023
Published: 11 April 2023



## 1. Introduction

Basalt is the most widespread magmatic or igneous effusive rock. With andesite, another type of volcanic rock, it makes up almost all, about 98%, of the rocks made up of the lava that erupted on the Earth's surface and was then subjected to a process of crystallization. Generally, when not greatly weathered, basalt has colorations that from dark gray can tend to black [1]. For several years, it has been employed in casting procedures to produce ceramic plates and panels for architectural purposes [2]. In addition, fused basalt coatings for iron pipes show an extremely high abrasion strength in manufacturing operations [3]. Basalt is also used in many countries in the construction of highway and airport pavements [4], and it also finds application in organic farming, in the form of micronized rock flour, to revitalize and nourish soils and plants that have lost fertility, such as intensive and extensive farming that deplete soils of natural elements [5].

Furthermore, fragmented basalt aggregates, which are compact, finely grained, very dark green or black rocks produced when melted lava from the depths of the Earth's crust

ascends and crystallizes, are also recognized as a natural resource for the manufacturing of cheap and eco-friendly construction materials with acceptable strength and durability features, well suited to the framework of sustainable development [6,7]. In detail, the partial replacement of Portland cement with basalt aggregates in concrete, when available, can lead to a more cost-efficient solution [8].

Basaltic rock in Italy can be found close to the Mt. Etna volcano (eastern Sicily, Southern Italy) [9], the edifice of which grew on a sedimentary substrate more than 1.5 km thick [10]. The origin of Mt. Etna's magmatism is probably related to extensive melting of the mantle, according to what is reported in [11].

In the present paper, a multi-technique approach including the use of High-Purity Germanium (HPGe) $\gamma$-ray spectrometry, Inductively Coupled Plasma Mass Spectrometry (ICP-MS) and X-ray diffraction (XRD) was employed with the aim to evaluate the radioactivity (radium-226, thorium-232, potassium-40 and caesium-137) and the heavy metals (arsenic, cadmium, copper, mercury, nickel, lead, antimony, thallium and zinc) content of the investigated basalt aggregate for concrete, picked up in a surrounding area of the Mt. Etna volcano [12], and to relate the natural radionuclides' specific activity to its mineralogical composition.

Furthermore, in order to assess any possible radiological hazard for the population, the calculation of the alpha index ($I_\alpha$), the radium equivalent activity ($Ra_{eq}$), the absorbed $\gamma$-dose rate (D) and the annual effective dose equivalent outdoor ($AEDE_{out}$) and indoor ($AEDE_{in}$) was performed [13–15]. Of note, in Italy, the current legislation states that building materials or additives of natural igneous origin are subject to radiometric checking before being placed on the commercial market [16].

Finally, with the aim to estimate the level of environmental chemical pollution by the heavy metals, the Enrichment Factor (EF), Geo-accumulation Index ($I_{geo}$), Contamination Factor (CF) and Pollution Load Index (PLI) were assessed [17,18].

## 2. Materials and Methods

### *2.1. Sample Collection*

The GPS coordinates of the specimen location are 37.53247 (latitude) and 15.037817 (longitude) (Figure 1).

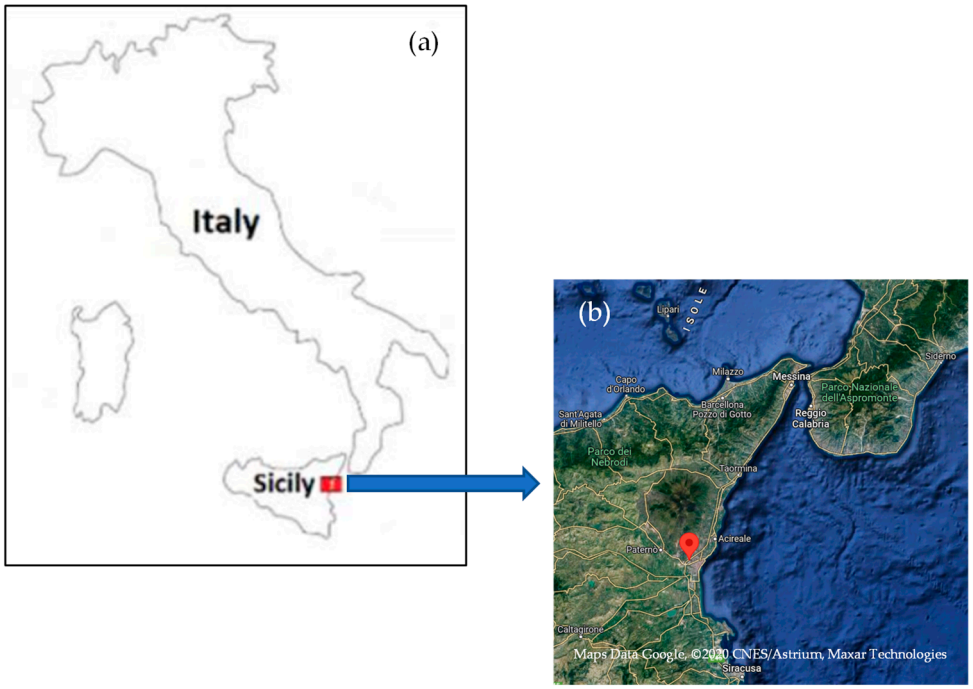


**Figure 1.** The sampling area (**a**), with the specimen location indicated (**b**).

Five aliquots of the basalt aggregate for concrete were collected in February 2022, from basalt outcrops, at depths of a few centimeters, and reduced to a coarse grain size by mechanical procedures. The sampling was performed from a relatively flat, clean, dry, hard surface, avoiding locations where surface dust or salts are likely to have accumulated.

After the collection, they were stored in labeled plastic containers, with proper precautions taken to avoid contamination [19], and subsequently transported to the laboratory.

### *2.2. HPGE γ-ray Spectrometry Measurements*

Each aliquot of the basalt aggregate for concrete was first dried, in order to completely remove the moisture and to obtain constant mass. After, it was inserted into a Marinelli hermetically sealed container of 250 mL capacity. After 40 days, the secular radioactive equilibrium between $^{226}$Ra and its daughter products was reached, and then the sample was ready for gamma spectrometry measurement with a live time of 70,000 s. Spectra were analyzed with the aim to assess the activity concentration of $^{226}$Ra, $^{232}$Th, $^{40}$K and $^{137}$Cs. In detail, the $^{226}$Ra activity concentration was calculated by using the 295.21 keV and 351.92 keV $^{214}$Pb and 1120.29 keV $^{214}$Bi gamma-ray lines, and the $^{232}$Th-specific activity was determined by using the 911.21 keV and 968.97 keV $^{228}$Ac γ-ray lines. In particular, for the $^{214}$Bi radionuclide, the TCS coincidence summation correction was applied [20] by using the MEFFTRAN code [21]. Continuing, for $^{40}$K, the evaluation was performed from its γ-line at 1460.8 keV and, finally, in order to investigate the anthropic radioactivity content, the $^{137}$Cs-specific activity was evaluated through its γ-line at 661.66 keV.

The experimental set-up was composed of a positive biased Ortec HPGe detector (GEM), whose operating parameters are reported in Table 1 [22].

**Table 1.** The HPGe GEM operating parameters.

| HPGe GEM | |
|---|---|
| **Parameter** | **Value** |
| Full Width at Half Maximum | 1.85 keV |
| Peak-to-Compton ratio | 64:1 |
| Relative Efficiency | 40% (at the 1.33 MeV $^{60}$Co γ-line) |
| Bias Voltage | 4500 V |
| Energy Range | 50 keV–2 MeV |

The detector was located inside lead wells to screen the environmental background radioactivity and, for efficiency and energy settings, a multi-peak Marinelli γ-source (BC-4464) of 250 mL capacity, energy range 60–1836 keV, custom made to replicate the exact designs of the specimens in a water-equivalent epoxy–resin matrix, was employed.

The Gamma Vision (Ortec) software was used for data acquisition and analysis [22].

The specific activity (Bq kg$^{-1}$ dry weight, d.w.) of the investigated radioisotopes was calculated as follows [23]:

$$C = \frac{N_E}{\varepsilon_E t \gamma_d M} \quad (1)$$

where $N_E$ is the net area of a peak at energy E; $\varepsilon_E$ and $\gamma_d$ are the efficiency and yield of the photopeak at energy E, respectively; M is the mass of the sample (kg); and t is the live time (s) [24]. Moreover, with the density of the basalt aggregate for concrete being higher than 1.1, the self-absorption correction on the activity concentration value was performed according to [25,26].

The Italian Accreditation Body (ACCREDIA) certified the quality of the γ-ray spectrometry experimental results [27], thus ensuring continuous verification that the performance properties of the method are preserved [28].

### *2.3. Evaluation of the Radiological Health Risk*

Several indexes developed over the years to evaluate the radiological risk for the human beings related to radiation exposure, i.e., the alpha index ($I_\alpha$), the radium equivalent activity ($Ra_{eq}$), the absorbed γ-dose rate (D) and the annual effective dose equivalent outdoor ($AEDE_{out}$) and indoor ($AEDE_{in}$), were calculated to estimate the potential radiation risk to humans.

#### 2.3.1. Alpha Index

The alpha index was calculated with the following formula [29]:

$$I_\alpha = C_{Ra}/200 \quad (2)$$

where $C_{Ra}$ is the mean activity concentrations of radium-226 in the basalt aggregate for concrete.

The alpha index allows to assess the alpha radiation exposure to the indoor radon exhaled from construction materials. The activity concentration of radium-226 must be lower than 200 Bq $kg^{-1}$, to prevent exposure to indoor radon-specific activity higher than the threshold value of 200 Bq $m^{-3}$ [16], and then $I_\alpha$ must be less than unity for the risk of exposure to radiation to be minimal.

#### 2.3.2. Radium Equivalent Activity

The radium equivalent activity is an index that describes the specific activities of radium-226, thorium-232 and potassium-40 in a single term [30,31]:

$$Ra_{eq}\ (Bq\ kg^{-1}) = C_{Ra} + 1.43C_{Th} + 0.077C_K \quad (3)$$

where $C_{Ra}$, $C_{Th}$ and $C_K$ are the mean activity concentrations of radium-226, thorium-232 and potassium-40 in the basalt aggregate for concrete, respectively.

This index must be lower than 370 Bq $kg^{-1}$ for the safe utilization of the basalt aggregate for concrete as building material [32].

#### 2.3.3. Absorbed γ-Dose Rate

This parameter was calculated with the following formula [33]:

$$D\ (nGy\ h^{-1}) = 0.462C_{Ra} + 0.604C_{Th} + 0.0417C_K \quad (4)$$

#### 2.3.4. Annual Effective Dose Equivalent Outdoor and Indoor

The annual effective dose equivalent for an individual was calculated using the equations below, with occupation factors of 20% and 80% for outdoor and indoor environments, respectively [34]:

$$AEDE_{out}\ (mSv\ y^{-1}) = D\ (nGy\ h^{-1}) \times 8760\ h \times 0.7\ Sv\ Gy^{-1} \times 0.2 \times 10^{-6} \quad (5)$$

$$AEDE_{in}\ (mSv\ y^{-1}) = D\ (nGy\ h^{-1}) \times 8760\ h \times 0.7\ Sv\ Gy^{-1} \times 0.8 \times 10^{-6} \quad (6)$$

Both must be lower than 1 mSv $y^{-1}$ for the radiological health risk to be negligible [16].

### *2.4. Inductively Coupled Plasma Mass Spectrometry (ICP-MS) Measurements*

For the ICP-MS analysis, approximately 0.5–1.0 g of sample, together with 3 mL of ultrapure (for trace analysis) $HNO_3$ (67–69%) and 9 mL of ultrapure (for trace analysis) HCl (32–35%) (aqua regia), was directly introduced into a 100 mL TFM vessel. A Milestone microwave system, Ethos 1, was used for the acid digestion, as follows: (i) 15 min at 1500 W and 180 °C; (ii) 10 min at 1500 W and 180 °C; (iii) 10 min at 1000 W and 120 °C, with 20 min cooling [35]. The mixture was filtered and filled to 50 mL with distilled $H_2O$ and diluted

10 times. Opportune dilutions of two certified materials were employed in order to prepare calibration solutions for the analytes in 0.5 % ($v/v$) $HNO_3$ and 0.5 % ($v/v$) HCl [18].

For the measurements, a Thermo Scientific iCAP Qc ICP-MS was used [36]. The instrument was operated in a single collision cell mode, with kinetic energy discrimination (KED), using pure He as the collision gas. All samples were presented for analysis using a Cetac ASX-520.

### *2.5. Evaluation of the Level of Heavy Metals Contamination*

In order to assess the level of heavy metals contamination in the basalt aggregate for concrete, the pollution indices reported in the following were calculated.

#### 2.5.1. The Enrichment Factor

This index was evaluated as follows [37]:

$$EF = \frac{\{C_x/C_{Fe}\}sample}{\{C_x/C_{Fe}\}reference} \quad (7)$$

where $C_x$ is the concentration of the potential enrichment element and $C_{Fe}$ is the concentration of the normalizing element, usually iron [37].

#### 2.5.2. The Geo-Accumulation Index

This pollution index is [38]:

$$I_{geo} = Log_2[C_n/(kB_n)] \quad (8)$$

where $C_n$ is the concentration of the potential harmful element in the sample, $B_n$ is the geochemical background value in the average shale of element n and k is the correction factor of the background matrix [38].

#### 2.5.3. The Contamination Factor

This index is given by [39]

$$CF = C_{metal}/C_{background} \quad (9)$$

where $C_{metal}$ and $C_{background}$ are the heavy metals concentration and background values, respectively [38].

#### 2.5.4. The Pollution Load Index

The n-th root of the product of the Contamination Factor of heavy metals is the Pollution Load Index [40]:

$$PLI = (CF_1 \times CF_2 \times CF_3 \times \ldots . \times CF_n)^{1/n} \quad (10)$$

where n is the number of metals [40].

### *2.6. XRD Analysis*

X-ray diffraction analyses were performed by using a Panalytical Empyrean Diffractometer with Cu $K_\alpha$ radiation on a Bragg–Brentano theta-theta goniometer, equipped with a solid-state detector, PIXcel [41].

The generator settings were 40 kV and 40 mA. The measurements were performed in glass slide holders ensuring a uniform dispersion of properly compressed specimens. The continuous scan mode was employed in order to span the 2Θ incidence angle from 5° to 60° with a scan velocity of 1.2° per minute. The total runtime for each analysis was about 45 min.

The observed peak positions were then compared with reference spectra from RRUFF database, with the aim to identify the crystalline mineralogical constituents of the analyzed basalt aggregate for concrete [42].

## 3. Results and Discussion

### *3.1. The Specific Activity of the Radioisotopes*

The average specific activity (the mean value of the 5 analyzed aliquots) of radium-226, thorium-232, potassium-40 and caesium-137, in the investigated basalt aggregate for concrete, was found to be (58.6 ± 6.6) Bq $kg^{-1}$ dry weight (d.w.), (40.7 ± 5.3) Bq $kg^{-1}$ d.w., (498 ± 57) Bq $kg^{-1}$ d.w. and lower than the minimum detectable activity (0.24 Bq $kg^{-1}$ d.w.), respectively. Table 2 reports the radium-226-, thorium-232-, potassium-40- and caesium-137-specific activity in the five analyzed aliquots, together with the average values.

**Table 2.** The specific activity $C_{Ra}$, $C_{Th}$, $C_K$ and $C_{Cs}$ of, respectively, $^{226}Ra$, $^{232}Th$, $^{40}K$ and $^{137}Cs$, in the five analyzed aliquots, together with the average values.

| Aliquot ID | $C_{Ra}$ (Bq $kg^{-1}$ d.w.) | $C_{Th}$ (Bq $kg^{-1}$ d.w.) | $C_K$ (Bq $kg^{-1}$ d.w.) | $C_{Cs}$ (Bq $kg^{-1}$ d.w.) |
|---|---|---|---|---|
| 1 | 53.6 ± 6.1 | 36.4 ± 4.9 | 498 ± 57 | <0.18 |
| 2 | 63.6 ± 7.1 | 44.9 ± 5.7 | 510 ± 66 | <0.24 |
| 3 | 58.6 ± 6.6 | 35.7 ± 5.1 | 491 ± 50 | <0.21 |
| 4 | 61.9 ± 6.8 | 45.7 ± 5.5 | 505 ± 64 | <0.27 |
| 5 | 55.3 ± 6.4 | 40.7 ± 5.3 | 486 ± 48 | <0.30 |
| Average | 58.6 ± 6.6 | 40.7 ± 5.3 | 498 ± 57 | <0.24 |

The worldwide average specific activity of radium-226, thorium-232 and potassium-40 is 35, 30 and 400 Bq $kg^{-1}$, respectively [32]. In light of this, the experimental results here reported show that, in our case, the average specific activity of all the detected radioisotopes is higher than the average worldwide value. These results need a more critical interpretation, which will be provided further below in terms of the mineralogical composition of the basalt aggregate for concrete itself.

Regarding caesium-137, the mean specific activity turned out to be lower than the minimum detectable activity, ruling out an anthropic contamination.

### *3.2. Radiological Hazard Effects Assessment*

With reference to the values of the radiological hazard indices, the alpha index, obtained by using Equation (2), was found to be 0.29, less than unity and thus avoiding exposure to the indoor radon concentration of more than 200 Bq $m^{-3}$. The radium equivalent activity was calculated through Equation (3) with the aim to ascertain the suitability of the investigated basalt aggregate for concrete for use as a structural material component. The obtained value was 155 Bq $kg^{-1}$, lower than 370 Bq $kg^{-1}$, set as the threshold limit for building materials, thus ensuring again that the analyzed sample may not be harmful if employed for civil construction.

The absorbed γ-dose rate, as obtained through Equation (4), was found to be equal to 65.3 nGy $h^{-1}$, a value attributable to the lithologic component of the sampling site [43], and it was used to evaluate, through Equations (5) and (6), the annual effective dose equivalent outdoor and indoor due to the activities of the radium-226, thorium-232 and potassium-40 in the investigated sample. The obtained values were 88.8 μSv $y^{-1}$ and 355 μSv $y^{-1}$, respectively, lower than the threshold value of 1 mSv $y^{-1}$ [16].

### *3.3. Heavy Metals Content*

Table 3 reports the heavy metals content (mg $kg^{-1}$ d.w.) for the analyzed basalt aggregate for concrete.

**Table 3.** Heavy metals content (mg $kg^{-1}$ d.w.) for the analyzed basalt aggregate for concrete.

| ICP-MS Analysis | | |
|---|---|---|
| | | *Threshold limit* |
| $C_{As}$ | 0.87 | 20 |
| $C_{Cd}$ | 0.03 | 2 |
| $C_{Cu}$ | 70.8 | 120 |
| $C_{Hg}$ | 0.04 | 1 |
| $C_{Ni}$ | 9.09 | 120 |
| $C_{Pb}$ | 8.90 | 100 |
| $C_{Sb}$ | 0.06 | 10 |
| $C_{Tl}$ | 0.02 | 1 |
| $C_{Zn}$ | 50.1 | 150 |

Of note, the obtained results are lower than the threshold limits [44]; hence, they can be regarded as no pollutants and do not compromise the well-being of the environment.

### *3.4. Evaluation of the Heavy Metals Contamination Level*

#### 3.4.1. EF

In agreement with [45], an EF < 2 indicates minimal enrichment. In particular, 0.5 < EF < 1.5 shows a natural-origin metal, while EF > 1.5 suggests a more likely anthropic one [45]. Moreover, the values between 2 and 5 indicate moderate enrichment; between 5 and 20, significant enrichment; between 20 and 40, high enrichment; and an EF higher than 40, extremely high enrichment.

The obtained EF values, reported in Table 4, were found to be <2 in all cases, indicating no or minimal enrichment.

**Table 4.** Calculated values of EF, $I_{geo}$, CF and PLI for the investigated sample.

| Metal | Index of Contamination | | | |
|---|---|---|---|---|
| | **EF** | **$I_{geo}$** | **CF** | **PLI** |
| As | 0.07 | −4.49 | 0.07 | |
| Cd | 0.10 | −3.91 | 0.10 | |
| Cu | 1.58 | 0.07 | 1.57 | |
| Hg | 0.10 | −3.91 | 0.10 | |
| Ni | 0.13 | −3.49 | 0.13 | 0.14 |
| Pb | 0.45 | −1.75 | 0.45 | |
| Sb | 0.04 | −5.23 | 0.04 | |
| Tl | 0.01 | −6.71 | 0.01 | |
| Zn | 0.53 | −1.51 | 0.53 | |

#### 3.4.2. $I_{geo}$

The $I_{geo}$ values must be interpreted as follows [46]:

$I_{geo} \leq 0$ denotes no contamination;
For $0 < I_{geo} \leq 1$, no/a medium degree of contamination;
For $1 < I_{geo} \leq 2$, a medium degree of contamination;
For $2 < I_{geo} \leq 3$, a medium/high degree of contamination;
For $3 < I_{geo} \leq 4$, a high degree of contamination;
For $4 < I_{geo} \leq 5$, a high/very high degree of contamination;
$I_{geo} > 5$, a very high degree of contamination.

The obtained $I_{geo}$ values, reported in Table 4, were found to be <0 with the only exception being copper, probably because it is often used as a soil defense product, as well as the soil texture and its high pH [46,47].

#### 3.4.3. CF

According to [47], a CF $\leq$ 1 indicates no contamination; 1 < CF $\leq$ 3, a low or medium degree of contamination; 3 < CF $\leq$ 6, a high degree of contamination; and CF > 6, a very high degree of contamination.

The obtained CF values, reported in Table 4, are <1 in all cases except copper, showing again a very moderate degree of contamination for this metal.

#### 3.4.4. PLI

According to [48], a PLI value higher than 1 indicates chemical pollution.

In our case, the PLI was found to be <1, thus revealing no pollution by the investigated heavy metals.

### *3.5. XRD Analysis*

The X-ray diffraction analysis result is shown in Figure 2.

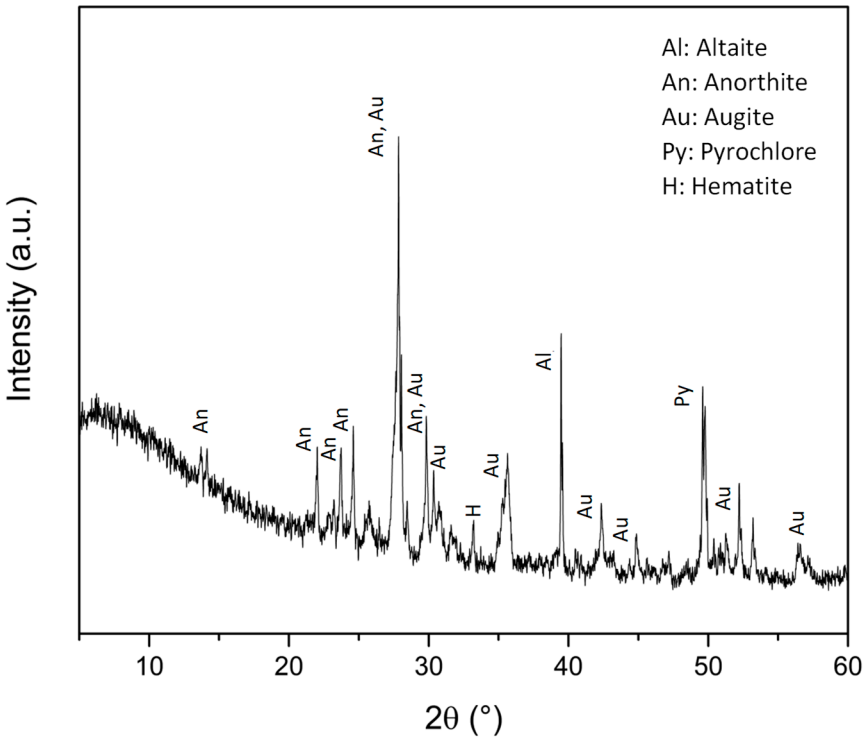


**Figure 2.** The X-ray diffraction analysis of the investigated basalt aggregate for concrete.

Minerals recognition was performed by comparing the measured diffraction peak positions to the RRUFF database. An XRD analysis put in evidence the presence of Altaite (PbTe, RRUFF ID: R060939), Anorthite ($Ca(Al_2Si_2O_8)$, RRUFF ID: R040059), Augite ($(Ca,Mg,Fe)_2Si_2O_6$, RRUFF ID: R061108), Pyrochlore ((Na,Ca)2Nb2O6(OH,F), RRUFF ID: R060151) and Hematite ($Fe_2O_3$, RRUFF ID: R040024), superimposed to a glassy groundmass, in the investigated basalt aggregate for concrete.

Of note, we can reliably hold the detected mineralogical phases to account for the radionuclides content previously discussed. In particular, the high specific activity of radium-226, thorium-232 and potassium-40 radioisotopes, if compared with the average worldwide value, can be explained taking into account that, from the diffractogram, it is possible to evince in particular the presence of pyrochlore, in the composition of which

Niobium appears. This REE represents an element that, from a geochemical point of view, is a marker of occurrence of crustal contamination, i.e., a migration of isotopes of various elements from the Earth's crust to the magma, which then solidified and became basalt [49,50]. Therefore, in light of this, it is possible to justify the specific activity values of the detected natural radioisotopes, which are higher than the average worldwide value in all cases [51].

## 4. Conclusions

The natural and anthropic radioactivity content of a basalt aggregate for concrete from Sicily, Southern Italy, was analyzed through High-Purity Germanium (HPGe) $\gamma$-ray spectrometry. Moreover, calculations of the alpha index ($I_\alpha$), the radium equivalent activity ($Ra_{eq}$), the absorbed $\gamma$-dose rate (D) and the annual effective dose equivalent outdoor ($AEDE_{out}$) and indoor ($AEDE_{in}$) were performed in order to estimate the radiological hazard for human beings. Of note, the obtained values turned out to be lower than the maximum recommended ones for humans, thereby rationally excluding any significant health impact related to exposure to ionizing radiation. Additionally, the mean specific activity of caesium-137 turned out to be lower than the minimum detectable activity.

Next, the concentration levels of the heavy metals in the analyzed basalt aggregate for concrete were investigated through Inductively Coupled Plasma Mass Spectrometry (ICP-MS). The resulting values were found to be below the threshold levels established by Italian legislation and thus do not reasonably represent a health risk to humans. In addition, the calculation of various pollution indices was carried out in order to assess the ecological risk from heavy metals imposed on the ecology of the ecosystem. The obtained results show a very minimal enrichment only for copper, probably due to the use of this metal as a soil defense product, as well as the soil texture and its high pH, and in general no pollution by the assessed heavy metals.

Finally, X-ray diffraction (XRD) was applied to recognize the mineralogical/geochemical composition of the investigated sample and to relate it to the natural radioactivity content. From the results, we can conclude that the analyzed basalt aggregate for concrete was characterized by the presence of Altaite, Anorthite, Augite, Pyrochlore and Hematite, superimposed to a glassy groundmass. Moreover, the natural radionuclides' specific activity reported in the present study underlined a high value of the activity concentration of radium-226, thorium-232 and potassium-40 radionuclides with respect to the average worldwide value. This can be explained by the occurrence of crustal contamination, put in evidence by the presence, in the diffractogram, of pyrochlore, in the composition of which Niobium appears.

**Author Contributions:** Conceptualization, F.C. and V.V.; methodology, F.C. and G.P.; validation, D.M.; formal analysis, A.B., M.D., S.M. and M.M.; investigation, F.C. and V.V.; resources, F.C. and V.C.; data curation, F.C.; writing—original draft preparation, F.C.; supervision, D.M. and V.V. All authors have read and agreed to the published version of the manuscript.

**Funding:** This research received no external funding.

**Institutional Review Board Statement:** Not applicable.

**Informed Consent Statement:** Not applicable.

**Conflicts of Interest:** Authors declare no conflict of interest.

## References

1. Reino, W.; Pucha, G.; Recalde, C.; Tene, T.; Cadena, P. Occurrence of radioactive materials in pyroclastic flows of Tungurahua volcano using gamma spectrometry. *AIP Conf. Proc.* **2018**, *2003*, 020014. [CrossRef]
2. Kerur, B.; Tanakanti, R.; Basappa, D.; Kumar, A.; Narayani, K.; Rekha, A.; Hanumaiah, B. Radioactivity levels in rocks of North Karnataka, India. *Indian J. Pure Appl. Phys.* **2010**, *48*, 809–812.
3. Malczewski, D.; Dziurowicz, M.; Kalab, Z.; Rösnerová, M. Natural radioactivity of rocks from the historic Jeroným Mine in the Czech Republic. *Environ. Earth Sci.* **2021**, *80*, 650. [CrossRef]

4. Faanu, A.; Adukpo, O.K.; Tettey-Larbi, L.; Lawluvi, H.; Kpeglo, D.O.; Darko, E.O.; Emi-Reynolds, G.; Awudu, R.A.; Kansaana, C.; Amoah, P.A.; et al. Natural radioactivity levels in soils, rocks and water at a mining concession of Perseus gold mine and surrounding towns in Central Region of Ghana. *Springerplus* **2016**, *5*, 98. [CrossRef]
5. Conceição, L.T.; Silva, G.N.; Holsback, H.M.S.; Oliveira, C.d.F.; Marcante, N.C.; Martins, É.d.S.; Santos, F.L.d.S.; Santos, E.F. Potential of basalt dust to improve soil fertility and crop nutrition. *J. Agric. Food Res.* **2022**, *10*, 100443. [CrossRef]
6. Caridi, F.; Torrisi, L.; Mezzasalma, A.M.; Mondio, G.; Borrielli, A. $Al_2O_3$ plasma production during pulsed laser deposition. *Eur. Phys. Journ. D* **2009**, *54*, 467–472. [CrossRef]
7. Zagorodnyuk, L.H.; Mestnikov, A.E.; Makhortov, D.S.; Akhmed, A.A.A. Mixed binders with the use of volcanic ash. *Lect. Notes Civ. Eng.* **2021**, *95*, 9–15. [CrossRef]
8. Ahmedai, M.A.; Ahmed, S.A.; Ahmed, Y.H.; Ibrahiem, E.S.M. Tagabo Volcanic Ash as Cement Replacing Materials. *FES J. Eng. Sci.* **2021**, *9*, 35–39. [CrossRef]
9. Chester, D.K.; Duncan, A.M.; Guest, J.E.; Kilburn, C.R.J. Mount Etna. The Anatomy of a Volcano. *Geol. Mag.* **1986**, *123*, 463–464. [CrossRef]
10. Tanguy, J.-C.; Condomines, M.; Kieffer, G. Evolution of the Mount Etna magma: Constraints on the present feeding system and eruptive mechanism. *J. Volcanol. Geotherm. Res.* **1997**, *75*, 221–250. [CrossRef]
11. Gvirtzman, Z.; Nur, A. The formation of Mount Etna as the consequence of slab rollback. *Nature* **1999**, *401*, 782–785. [CrossRef]
12. Kozłowska, B.; Walencik-łata, A.; Giammanco, S.; Immè, G.; Catalano, R.; Mangano, G. Radioactivity of mt. Etna volcano and radionuclides transfer to groundwater. *Ann. Geophys.* **2019**, *62*, 1–12. [CrossRef]
13. Caridi, F.; D'Agostino, M.; Messina, M.; Marcianò, G.; Grioli, L.; Belvedere, A.; Marguccio, S.; Belmusto, G. Lichens as environmental risk detectors. *Eur. Phys. J. Plus* **2017**, *132*, 189. [CrossRef]
14. Caridi, F.; D'Agostino, M.; Belvedere, A.; Marguccio, S.; Belmusto, G. Radon radioactivity in groundwater from the Calabria region, south of Italy. *J. Instrum.* **2016**, *11*, P05012. [CrossRef]
15. Avwiri, G.O.; Egieya, J.M. Radiometric assay of hazard indices and excess lifetime cancer risk due to natural radioactivity in soil profile in Ogba/Egbema/Ndoni local government area of Rivers state, Nigeria. *Acad. Res. Int.* **2013**, *4*, 54–65.
16. Italian Legislation D.Lgs. 101/20. Available online: https://www.normattiva.it/ (accessed on 20 February 2023).
17. Caridi, F.; Messina, M.; D'Agostino, M. An investigation about natural radioactivity, hydrochemistry, and metal pollution in groundwater from Calabrian selected areas, southern Italy. *Environ. Earth Sci.* **2017**, *76*, 668. [CrossRef]
18. Mottese, A.F.; Fede, M.R.; Caridi, F.; Sabatino, G.; Marcianò, G.; Calabrese, G.; Albergamo, A.; Dugo, G. Chemometrics and innovative multidimensional data analysis (MDA) based on multi-element screening to protect the Italian porcino (Boletus sect. Boletus) from fraud. *Food Control* **2020**, *110*, 107004. [CrossRef]
19. Stewart, C.; Horwell, C.; Plumlee, G.; Cronin, S.; Delmelle, P.; Baxter, P.; Calkins, J.; Damby, D.; Morman, S.; Oppenheimer, C. *Protocol for Analysis of Volcanic Ash Samples for Assessment of Hazards from Leachable Elements*; International Volcanic Health Hazard Network Publisher: Durham, UK, 2013; pp. 1–22.
20. Agarwal, C.; Chaudhury, S.; Goswami, A.; Gathibandhe, M. True coincidence summing corrections in point and extended sources. *J. Radioanal. Nucl. Chem.* **2011**, *289*, 773–780. [CrossRef]
21. Available online: https://efftran.github.io/ (accessed on 20 February 2023).
22. Caridi, F.; Marguccio, S.; Durante, G.; Trozzo, R.; Fullone, F.; Belvedere, A.; D'Agostino, M.; Belmusto, G. Natural radioactivity measurements and dosimetric evaluations in soil samples with a high content of NORM. *Eur. Phys. J. Plus* **2017**, *132*, 56. [CrossRef]
23. Caridi, F.; Messina, M.; Belvedere, A.; D'Agostino, M.; Marguccio, S.; Settineri, L.; Belmusto, G. Food salt characterization in terms of radioactivity and metals contamination. *Appl. Sci.* **2019**, *9*, 2882. [CrossRef]
24. Caridi, F.; Di Bella, M.; Sabatino, G.; Belmusto, G.; Fede, M.R.; Romano, D.; Italiano, F.; Mottese, A.F. Assessment of Natural Radioactivity and Radiological Risks in River Sediments from Calabria (Southern Italy). *Appl. Sci.* **2021**, *11*, 1729. [CrossRef]
25. Caridi, F.; Marguccio, S.; Belvedere, A.; D'Agostino, M.; Belmusto, G. A methodological approach to a radioactive sample analysis with low-level $\gamma$-ray spectrometry. *J. Instrum.* **2018**, *13*, P09022. [CrossRef]
26. Torrisi, L.; Caridi, F.; Margarone, D.; Borrielli, A. Plasma-laser characterization by electrostatic mass quadrupole analyzer. *Nucl. Instr. Meth. Phys. Res. B.* **2008**, *266*, 308–315. [CrossRef]
27. ACCREDIA. Available online: https://www.accredia.it/ (accessed on 13 February 2023).
28. Caridi, F.; D'Agostino, M.; Belvedere, A. Radioactivity in calabrian (Southern Italy) wild boar meat. *Appl. Sci.* **2020**, *10*, 3580. [CrossRef]
29. Xinwei, L. Radioactivity level in Chinese building ceramic tile. *Radiat. Prot. Dosim.* **2004**, *112*, 323–327. [CrossRef]
30. Caridi, F.; Testagrossa, B.; Acri, G. Elemental composition and natural radioactivity of refractory materials. *Environ. Earth Sci.* **2021**, *80*, 170. [CrossRef]
31. Caridi, F.; Paladini, G.; Venuti, V.; Crupi, V.; Procopio, S.; Belvedere, A.; D'agostino, M.; Faggio, G.; Grillo, R.; Marguccio, S.; et al. Radioactivity, metals pollution and mineralogy assessment of a beach stretch from the ionian coast of calabria (Southern italy). *Int. J. Environ. Res. Public Health* **2021**, *18*, 12147. [CrossRef]
32. United Nations Scientific Committee on the Effects of Atomic Radiation. *Sources and Effects of Ionizing Radiation: Report to the General Assembly, with Scientific Annexes*; United Nations Scientific Committee on the Effects of Atomic Radiation: Vienna, Austria, 2000; Volume I, ISBN 92-1-142238-8.

33. Caridi, F.; Marguccio, S.; Belvedere, A.; Belmusto, G.; Marcianò, G.; Sabatino, G.; Mottese, A. Natural radioactivity and elemental composition of beach sands in the Calabria region, south of Italy. *Environ. Earth Sci.* **2016**, *75*, 629. [CrossRef]
34. Caridi, F.; D'Agostino, M.; Belvedere, A.; Marguccio, S.; Belmusto, G.; Gatto, M.F. Diagnostics techniques and dosimetric evaluations for environmental radioactivity investigations. *J. Instrum.* **2016**, *11*, C10012. [CrossRef]
35. Hassan, N.M.; Rasmussen, P.E.; Dabek-Zlotorzynska, E.; Celo, V.; Chen, H. Analysis of Environmental Samples Using Microwave-Assisted Acid Digestion and Inductively Coupled Plasma Mass Spectrometry: Maximizing Total Element Recoveries. *Water. Air. Soil Pollut.* **2007**, *178*, 323–334. [CrossRef]
36. Thermo Fisher. *iCAP Q Operating Manual*; Thermo Fisher: Waltham, MS, USA, 2012.
37. Turekian, K.K.; Haven, N.; Hans, K.; Universitat, W.M. Der Distribution of the Elements in Some Major Units of the Earth's Crust. *America* **1961**, *72*, 175–192.
38. Håkanson, L. An Ecological Risk Index for Aquatic Pollution Control—A Sedimentological Approach. *Water Res.* **1980**, *14*, 975–1001. [CrossRef]
39. Chandrasekaran, A.; Ravisankar, R.; Harikrishnan, N.; Satapathy, K.K.; Prasad, M.V.R.; Kanagasabapathy, K.V. Multivariate statistical analysis of heavy metal concentration in soils of Yelagiri Hills, Tamilnadu, India–Spectroscopical approach. *Spectrochim. Acta Part A Mol. Biomol. Spectrosc.* **2015**, *137*, 589–600. [CrossRef]
40. Ramasamy, V.; Meenakshisundaram, V.; Venkatachalapathy, R.; Ponnusamy, V. Influence of mineralogical and heavy metal composition on natural radionuclide concentrations in the river sediments. *Appl. Radiat. Isot.* **2011**, *69*, 1466–1474. [CrossRef]
41. Malvern Panalytical. *Empyrean Diffractometer User Manual*; Malvern Panalytical: Malvern, UK, 2013.
42. Available online: https://rruff.info (accessed on 20 February 2023).
43. Morelli, D.; Immé, G.; Cammisa, S.; Catalano, R.; Mangano, G.; La Delfa, S.; Patanè, G. Radioactivity measurements in volcano-tectonic area for geodynamic process study. *Eur. Phys. J. Web Conf.* **2012**, *24*, 05009.
44. D. Lgs. 152/2006. Available online: https://www.normattiva.it/ (accessed on 20 February 2023).
45. Zheng, L.-G.; Liu, G.-J.; Kang, Y.; Yang, R.-K. Some potential hazardous trace elements contamination and their ecological risk in sediments of western Chaohu Lake, China. *Environ. Monit. Assess.* **2010**, *166*, 379–386. [CrossRef]
46. Karimi, B.; Masson, V.; Guilland, C.; Leroy, E.; Pellegrinelli, S.; Giboulot, E.; Maron, P.-A.; Ranjard, L. Ecotoxicity of copper input and accumulation for soil biodiversity in vineyards. *Environ. Chem. Lett.* **2021**, *19*, 2013–2030. [CrossRef]
47. Pietrzak, U.; McPhail, D.C. Copper accumulation, distribution and fractionation in vineyard soils of Victoria, Australia. *Geoderma* **2004**, *122*, 151–166. [CrossRef]
48. Naji, A.; Ismail, A. Assessment of Metals Contamination in Klang River Surface Sediments by using Different Indexes. *Environ. Asia* **2011**, *4*, 30–38. [CrossRef]
49. Gołuchowska, K.; Barker, A.K.; Manecki, M.; Majka, J.; Kośmińska, K.; Ellam, R.M.; Bazarnik, J.; Faehnrich, K.; Czerny, J. The role of crustal contamination in magma evolution of Neoproterozoic metaigneous rocks from Southwest Svalbard. *Precambrian Res.* **2022**, *370*, 106521. [CrossRef]
50. Catalano, S.; Torrisi, S.; Ferlito, C. The relationship between Late Quaternary deformation and volcanism of Mt. Etna (eastern Sicily): New evidence from the sedimentary substratum in the Catania region. *J. Volcanol. Geotherm. Res.* **2004**, *132*, 311–334. [CrossRef]
51. Li, X.; Li, J.; Bader, T.; Mo, X.; Scheltens, M.; Chen, Z.; Xu, J.; Yu, X.; Huang, X. Evidence for crustal contamination in intra-continental OIB-like basalts from West Qinling, central China: A Re–Os perspective. *J. Asian Earth Sci.* **2015**, *98*, 436–445. [CrossRef]